



INFLUENCE OF MICROSTRUCTURAL FEATURES ON THE CORROSION BEHAVIOUR OF AZ91 ALLOY IN CHLORIDE MEDIA

Lenka Bukovinová^{1,*}, Michal Bukovina¹, Filip Pastorek²

¹ Research Centre, University of Žilina, Univerzitná 8215/1, 010 26 Žilina, Slovakia

² Department of Materials Engineering, Faculty of Mechanical Engineering, University of Žilina, Univerzitná 8215/1, 010 26 Žilina, Slovakia

* corresponding author: e-mail: lenka.bukovinova@rc.uniza.sk

Resume

The corrosion resistance of materials is dependent also on their microstructure. Microstructural parts can have different electrochemical properties as the basic material. This is the cause of the inductive current formation in the structure which has a negative effect on the corrosion resistance of materials. The influence of the microstructure of a cast AZ91 magnesium alloy, to which the solution annealing treatment and the ageing treatment was applied, was evaluated in terms of its corrosion behaviour in 0.1 M NaCl solution at room temperature. The corrosion process was monitored by electrochemical impedance spectroscopy (EIS) and the surface was characterized by scanning Kelvin probe force microscopy (SKPFM). The extent of corrosion damage was dependent on the microstructure. Surface potential maps indicated that, the surface potential of α -matrix is more negative than surface potential of $Mg_{17}Al_{12}$ phase.

Article info

Article history:

Received 28 December 2013

Accepted 2 June 2014

Online 26 November 2014

Keywords:

AZ91 alloy;
Solid solution;
 $Mg_{17}Al_{12}$ phase;
EIS;
AFM.

Available online: <http://fstroj.uniza.sk/journal-mi/PDF/2014/21-2014.pdf>

ISSN 1335-0803 (print version)

ISSN 1338-6174 (online version)

1. Introduction

Magnesium alloys are experiencing increased use in present automobile due to their capacity for vehicle lightweighting, specifically in structural components. The decreased mass offered by magnesium alloys allows for increased fuel efficiency and decreased greenhouse gas emissions. With a specific stiffness and strength comparable to steels, magnesium alloys also offer ease of castability [1 - 3], (especially in high pressure die-casting (HPDC)), good machinability, and reclamation. There is an urge to save weight at the front axle, especially on front-wheel drive vehicles [4]. Unfortunately, the high reactivity and poor corrosion resistance have to a great extent limited the application of magnesium alloys in industry. There are two main reasons for the poor corrosion resistance of many magnesium alloys: (1) internal galvanic

corrosion caused by second phases such as $Mg_{17}Al_{12}$, AlMn, $Al_{18}Mn_5$, $Mg_{12}Nd$ and Mg_2Pb or impurities; (2) the oxide/hydroxide film on magnesium is much less protective than the film on a conventional metal, such as aluminum or stainless steel. The surface film on magnesium or a magnesium alloy has low corrosion resistance [5]. AZ91 alloy is the most favored magnesium alloy, being used in approximately 90 % of all magnesium cast products [6, 7]. Compared with the sand casted AZ91, the microstructure of the high pressure die-cast AZ91 alloy is finer and more homogenous. Residual microstructure stress was left during the HPDC process. The manufacturing processes for Mg alloy components have a great influence on the morphology, size, and distribution of the phases in the alloy, which lead to differences in their corrosion behaviour. With the increase

of outdoor HPDC Mg alloy component use, the atmospheric influence on the corrosion processes should not be ignored [8]. AZ91 alloy has a two-phase microstructure typically consisting of a matrix of α -Mg solid solution with an intermetallic β -phase ($\text{Mg}_{17}\text{Al}_{12}$) along the grain boundaries. The physical significance of aluminum as the alloying element is largely related to an increased passivity of the oxide film formed on the surface. However, it seems that a threshold of 4 % Al in the alloy is required [9, 10]. β - $\text{Mg}_{17}\text{Al}_{12}$ has a more positive corrosion potential than the α -magnesium phase and may accelerate galvanic corrosion of α -magnesium (matrix). β - $\text{Mg}_{17}\text{Al}_{12}$ can also act as a corrosion barrier and hinder corrosion propagation in the matrix. β - $\text{Mg}_{17}\text{Al}_{12}$ could reduce the corrosion rate of AZ91 by forming a corrosion-resistant barrier through the precipitation of an Al-rich coring structure along grain boundaries. The eutectic ($\alpha+\beta$) and α -magnesium (matrix) phases have different aluminium contents. Therefore, it has been suggested that they may have different electrochemical behaviours. Both α -magnesium and the eutectic phase could form galvanic corrosion with the β - $\text{Mg}_{17}\text{Al}_{12}$ phase [11, 12]. The corrosion resistance of materials is dependent also on their microstructure. Microstructural parts of the phases can have different electrochemical properties as the base matrix. This is the cause of the inductive current formation in the structure which has a negative effect on the corrosion resistance of materials.

The paper deals with the influence of microstructural parts on the corrosion resistance of AZ91 magnesium alloy. Corrosion characteristics were measured using electrochemical impedance spectroscopy (EIS) method in a standard 0.1 M NaCl solution at 22 °C. The results of EIS measurements are supplemented by measurements of surface potential of structural parts of the atomic force microscope using the scanning Kelvin probe force microscopy (SKPFM) mode.

2. Experimental material and procedure

All experiments were performed on an AZ91 magnesium alloy (chemical composition in wt %: Al: 8.12, Zn: 0.68, Mn: 0.37, Si: 0.08, Cu: 0.03, Fe: 0.01, Ni: 0.009, Be: 0.003, and balance Mg) after continuous casting. Conventional heat treatment, involving solution annealing at about 413 °C for 16 h, followed by ageing at about 168 °C for 8 h, was applied after casting.

The microstructure of tested alloy was analyzed by Carl ZEIS AXIO Imager.A1m optical microscope after routine metallographic preparation. The microstructure of AZ91 magnesium alloy (Fig. 1) with aluminum additives of about 9wt.% consisted of primary α grains surrounded by a eutectic mixture of α and β ($\text{Mg}_{17}\text{Al}_{12}$) [3].

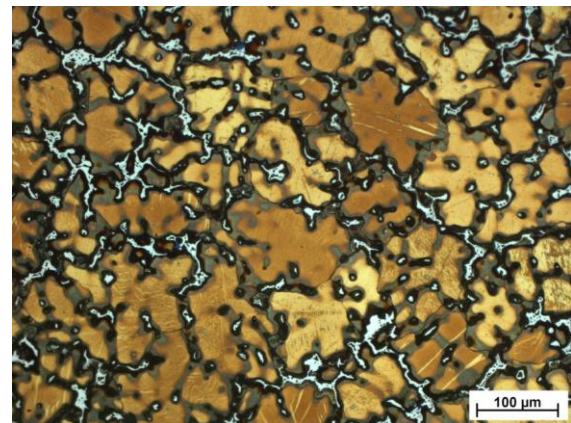


Fig. 1. Microstructure of AZ91 magnesium alloy, light microscopy (polarized light), etch. 2% Nital. (full colour version available online)

Electrochemical impedance spectroscopy

Electrochemical impedance measurements were conducted in 0.1 M NaCl after different times up to 96 hours at room temperature (22 ± 2 °C). For this purpose, VSP laboratory equipment produced by BioLogic SAS France with EC-Lab V10.12 software was used. The frequency ranged from 100 kHz to 50 mHz with 10 points/decade, whereas the amplitude of the sinusoidal potential signal was 10 mV with respect to the open circuit potential (OCP) at the beginning of each

measurement. A saturated calomel electrode and a platinum electrode served as the reference and auxiliary electrodes, respectively. AZ91 specimens formed the working electrode (a classical three electrode system) in such a way that only 1cm^2 area of the working electrode surface was exposed to the electrolyte solution in corrosion cell [13].

Electrochemical impedance spectroscopy is an experimental technique in which sinusoidal modulation of an input signal is used to obtain the transfer function for an electrochemical system. In its usual application, the modulated input is potential, the measured response is current, and the transfer function is represented as impedance. The impedance is obtained at different modulation frequencies, thus invoking the term spectroscopy. Through use of system-specific models, the impedance response can be interpreted in terms of kinetic and transport parameters [14].

Scanning Kelvin probe force microscopy

Scanning Kelvin probe force microscopy was used to acquire information about the local nobility of the different microstructural phases on the submicron scale. The SKPFM technique is a non-destructive procedure for measuring the surface distribution of the Volta potential [15]. A commercial atomic force microscope SOLVER NEXT by NT-MDT Co. was used. Kelvin probe force microscopy (Kelvin mode of Scanning Probe Microscopy) was used for measuring contact potential difference between the probe and the specimen. At present time Kelvin mode is based on the two-pass technique. In the first pass the topography is acquired using standard Semicontact mode. In the second pass this topography is retraced at a set lift height from the specimen surface to detect the Volta potential [16].

ô

3. Results and discussion

Fig. 2 discloses the Nyquist plots of cast AZ91 alloy after immersion in 0.1 M NaCl for several immersion times up to 96 hours. All diagrams reveal a capacitive loop at high and medium frequencies (HF and MF). Its diameter being associated with the charge-transfer resistance and, subsequently, with the corrosion resistance. At low frequencies (LF), a second loop or tail in the Nyquist plots reveals an inductive behaviour for all immersion times, except exposure time of 48 hours, when a mixed corrosion mechanism occurs (chemical reaction coupled with the formation of the layer of corrosion products which limits the activity of corrosion microcells by its existence and its morphology). Possibly, the diffusion of active components to the substrate was limited by the corrosion film layer.

Fig. 3 shows the equivalent circuit used to explain the corrosion behaviour of the tested alloy and for analysis of the electrochemical results. The circuit is composed of the electrolyte solution resistance (R_s) (very small in all cases) in series with the parallel RLQ circuit representing the electrical elements of the material. The HF/MF loop was simulated to a first approximation by a semicircle characteristic of the charge-transfer resistance (R_{CT}) of the corrosion reaction and the constant phase element (Q). The constant phase element was introduced into the circuit instead of the ideal double-layer capacitance or oxide film capacitance [15, 17]. When we add the coil (L) with its resistance (R_L) to the RQ circuit, we obtain the approximation for LF loop with the inductive nature of the alloy. The inductive loop is caused by the corrosion cells on the material surface. They can accrue among structural compounds in the microstructure of the material or among corrosion products and the material [17].

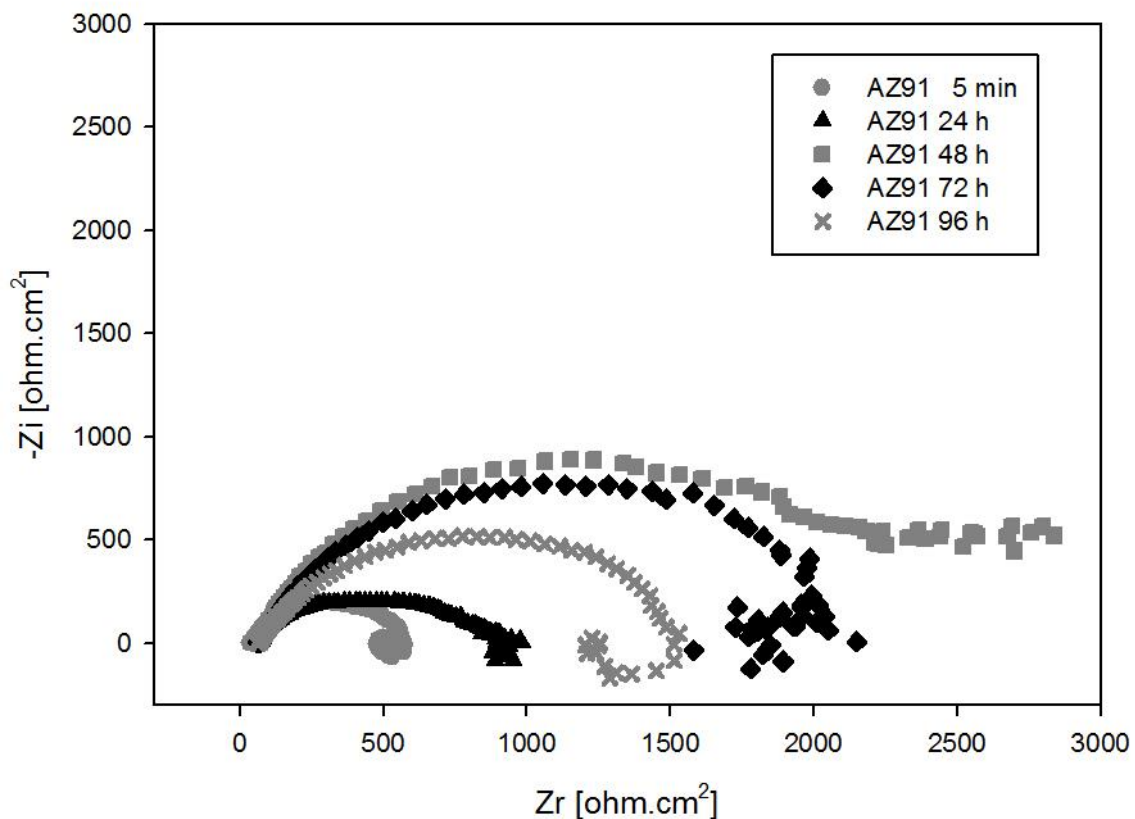


Fig. 2. Nyquist diagrams of AZ91 magnesium alloy in 0.1 M NaCl solution.

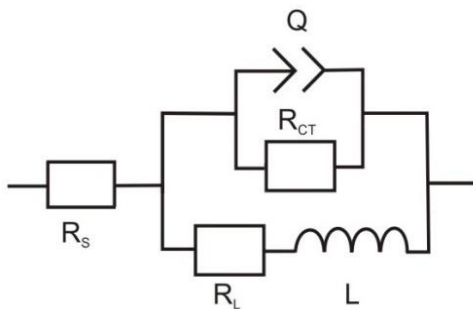
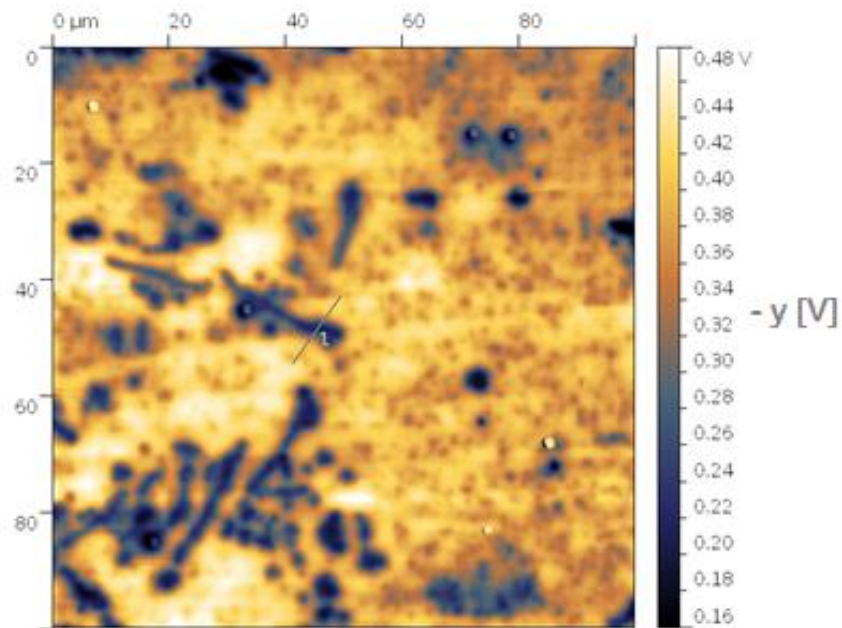


Fig. 3. Equivalent circuit model for analysis of Nyquist plots of AZ91 magnesium alloy.

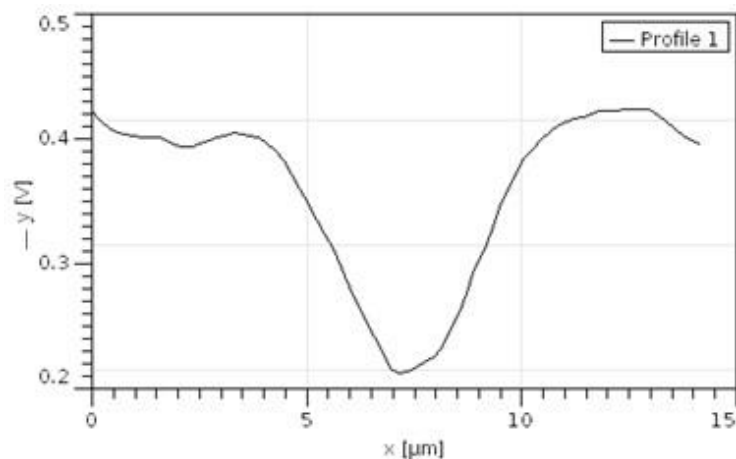
According to the analysis of Nyquist diagrams and measured polarization resistances, we are able to observe (Fig. 2) that after 24 or 48 hours of immersion in the corrosive media the R_p values doubled and quadrupled their size in comparison to the value of polarization resistance after

5 minutes of immersion. A curve resulting from measurements lasting 48 hours after immersion shows especially a change of its shape, which indicates a different corrosion mechanism after this immersion time. The corrosion is controlled by charge transfer (chemical reaction) for 96 hours. The curve with an inductive loop (values on imaginary axis below 0) reduces the values of polarization resistances. The decrease of polarization resistance values after 72 and 96 hours against the R_p value after 48 hours is caused by dropping out of protective corrosion products resulting in further active development of corrosion process.

We decided to verify the theory of corrosion cells formation between the α -matrix and β -phase using AFM microscopy by SKPFM mode.



a) Surface potential map.
(full colour version available online)



b) Profile-line analysis of potential.
Fig. 4. SKPFM study for AZ91 alloy.

Fig. 4a shows the map of surface potentials between solid solution (α) of AZ91 magnesium alloy and intermetallic phases (β) after metallographic preparation. Fig. 4b shows the surface potential through the line 1 indicated in Fig. 4a. It is obvious from the process that the surface potential of the α -matrix is more negative (approximately 200 mV) than surface potential of the β phase. The β -phase acts as an efficient cathode with

a strong galvanic couple at the β -phase/surrounding material interface [18]. This result confirmed the theory about structural features with different electrochemical properties. Individual structural features behave as corrosion cells causing faster material degradation in corrosive media. Therefore, it is clear that the microstructure of AZ91 alloy plays an important role in the corrosion mechanism of the tested magnesium alloy.

4. Conclusions

The corrosion behaviour of the cast AZ91 magnesium alloy followed by solution annealing and ageing was investigated using the electrochemical impedance spectroscopy (EIS) in 0.1. M NaCl solution and scanning Kelvin probe force microscopy (SKPFM) at room temperature. The following conclusions were emphasized:

- The theory about the presence of structural features with different electrochemical properties compare to the matrix was confirmed using metallographic analysis, EIS and SKPFM method.

- The corrosion is controlled by charge transfer (chemical reaction) after 5 minutes, 24, 72, and 96 hours, while a mixed corrosion mechanism – charge transfer coupled with the formation of the layer of corrosion products limiting the activity of corrosion cells by its existence and its morphology - is observed after 48 hours.

- Mg₁₇Al₁₂ phase has two times higher Volta potential compared to the matrix. The corrosion cells are created on the specimen surface and decrease total corrosion resistance of the material. SKPFM analysis also suggested that the β-phase produces a galvanic couple with the surrounding magnesium, though it possibly acts as an efficient cathode.

Acknowledgement

The research is supported by European regional development fund and Slovak state budget by the project “Research centre of University of Žilina”, ITMS 26220220183 and the project ITMS 26220220121 (call OPVaV-2008/2.2/01-SORO).

References

- [1] J. P. Weiler, J. T. Wood: *J. Alloys Comp.* 537 (2012) 133–140.
- [2] L. Li, Y. Cheng, H., Y. Zhang: *Trans. Nonferrous Met. Soc. China* 18 (2008) 722-727.
- [3] J. Li, J. Xie, J. Jin, Z. Wang: *Trans. Nonferrous Met. Soc. China* 22 (2012) 1028-1034.
- [4] G. Tong, H. Liu, Y. Liu : *Trans. Nonferrous Met. Soc. China* 20 (2010) 336-340.
- [5] R. Hu, S. Zhang, J. Bu, Ch. Lin, G. Song: *Prog. Org. Coat.* 73 (2012) 129– 141.
- [6] H. Bayani, E. Saebnoori: *J. Rare Earth.* 27(2) (2009) 255-258.
- [7] K. M. Asl, A. Masoudi, F. Khomamizadeh: *Mater. Sci. Eng. A* 527 (2010) 2027–2035.
- [8] L. Yang, Y. Li, Y. Wei, L. Hou, Y. Li, Y. Tian: *Corros. Sci.* 52 (2010) 2188–2196.
- [9] M. Ö. Öteyaka, E. Ghali, R. Tremblay: *Int. J. Corros.* 2012 (2012) 10 p.
- [10] R. Mahmudi, F. Kabirian, Z. Nematollahi: *Mater. Des.* 32 (2011) 2583–2589.
- [11] H. Krawiec, S. Stanek, V. Vignal, J. Lelito, J.S. Suchy: *Corros. Sci.* 53 (2011) 3108–3113.
- [12] B. Hadzima, M. Janeček, P. Suchý, J. Muller, L. Wagner: *Mater. Sci. Forum* 584 (2008)994-999
- [13] F. Pastorek, B. Hadzima: *Mater. Eng.-Mater. Inz.* 20(2) (2013) 54-63.
- [14] M. E. Orazem, B. Tribollet: *Electrochemical Impedance Spectroscopy.* Wiley-Interscience, 2008.
- [15] A. Pardo, M.C. Merino, A.E. Coy, F. Viejo, R. Arrabal, S. Feliú Jr.: *Electrochim. Acta* 53 (2008) 7890–7902.
- [16] <http://www.ntmdt.com/spm-principles/view/kelvin-probe-microscopy>
- [17] L. Škublová, B. Hadzima, M. Bukovina, V. Škorik: *J. Machine Manufacturing* 49 (E3-E5) (2009) 18-22.
- [18] S. Mathieu, C. Rapin, J. Steinmetz, P. Steinmetz: *Corros. Sci.* 45 (2003) 2741-2755.